CHINESE JOURNAL OF CATALYSIS
Volume 29, Issue 11, November 2008
Online English edition of the Chinese language journal

Available online at www.sciencedirect.com
ScienceDirect

Cite this article as: Chin J Catal, 2008, 29(11): 1138–1144.

RESEARCH PAPER

Selective Synthesis of Single/Double/Multi-walled Carbon Nanotubes on MgO-Supported Fe Catalyst

ZHANG Qiang, ZHAO Mengqiang, HUANG Jiaqi, QIAN Weizhong, WEI Fei*

Beijing Key Laboratory of Green Chemical Reaction Engineering and Technology, Department of Chemical Engineering, Tsinghua University, Beijing 100084, China

Abstract: By simple impregnation and hydrothermal treatment, MgO supported iron catalysts were obtained and used for carbon nanotube (CNT) growth from chemical vapor deposition with methane as the carbon source. Single/double/multi-walled CNTs (S/D/MWCNTs) were selectively synthesized on the Fe/MgO catalyst with different iron loadings. When the iron loading was low (0.5%), the iron atom distributed on the MgO support was sintered to iron nanoparticles with a size of 0.8–1.2 nm under the growth conditions. This catalyst promoted the formation of SWCNTs, which was attributed to the surface diffusion of carbon atoms on it. The selectivity for SWCNTs in the as-grown product from the 0.5%Fe/MgO catalyst was 90%, and the carbon mass yield was 19 times that of the active phase. When the iron loading was increased to 3%, larger iron catalyst particles of about 2.0 nm were formed. On this catalyst, there was more bulk diffusion of carbon, and DWCNTs became the main products due to the combination of both surface and bulk diffusion. With the iron loading was further increasing, iron particles from 1 to 8 nm were formed, which promoted the growth of MWCNTs together with S/DWCNTs. With increasing iron amount on the porous MgO support, the diameter, wall number, and proportion of semiconducting CNTs also increased. This provides a controllable way to selectively grow S/D/MWCNTs on a large scale in a fluidized bed to meet critical needs for CNTs in applications.

Key words: carbon nanotube; chemical vapor deposition; iron; magnesia; supported catalyst; microstructure; Raman spectroscopy

Carbon nanotubes (CNTs) have excellent electrical, thermal conductivity, and mechanical properties, and many potential applications in catalysis, composites, batteries, field emission displays, sensors, etc. [1–5]. The properties and applications can be different with different wall numbers and diameters. The first need in these applications is to produce high purity CNTs with a specific wall number on a large scale. The controlling of the wall number of CNTs has been a key issue for scientists and engineers. Chemical vapor deposition (CVD) has become the most important method to prepare single/double/multi-walled carbon nanotubes (S/D/MWCNTs). Metal catalysts, such as iron, nickel, and cobalt, are needed to crack hydrocarbons at the high temperature for CNT growth. The catalysts can be loaded on porous supports, substrates [6,7], or be formed in situ during CNT growth [8–11]. To meet the needs of large scale and high quality production at low cost, a fluidized bed is an ideal reactor for CNT growth [12]. A supported catalyst is needed in the process. At the moment, MWCNTs with a controlled diameter can be obtained on the ton scale [12]. However, the production of high quality S/DWCNTs on a large scale is still in progress. The active phase selection, catalyst preparation, and parameters for CNT synthesis have to be carefully considered and finely controlled. Among these factors, the catalyst is considered the key factor. Dal et al. [13] reported that SWCNTs can be obtained by the disproportionation of carbon monoxide at 1200 °C, with molybdenum particles as the catalyst. Later, Nikolaev et al. [14] found that Fe particles for SWCNT growth can be formed in situ by the thermal decomposition of iron pentacarbonyl in a flow of carbon monoxide at high pressure at 800–1200 °C. The high-pressure carbon monoxide process was developed soon after this [14]. Later, various groups found that SWCNTs or DWCNTs can be obtained on supported catalysts. At present, Fe, FeMo, and CoMo particles have been used as the active phase, and MgO, Al_2O_3,

Received date: 27 September 2008.
*** Corresponding author.** Tel: +86-10-62784654; Fax: +86-10-62772051; E-mail: weifei@flotu.org
Foundation item: Supported by the Foundation for the Author of National Excellent Doctoral Dissertation of China (200548), the National Natural Science Foundation of China (20606020), and the National Basic Research Program of China (973 Program, 2006CB0N0702).

SiO_2, and CaO as the supports. The synthesis of S/D/MWCNTs has been reported on Fe/Al_2O_3 [15,16], Fe/SiO_2 [17], Fe/MgO [18–25], $Fe/Mo/Al_2O_3$ [26,27], Fe/Mo/MgO [28–31], and Co/Mo/MgO [32,33] catalysts. The understanding of the selective growth of S/D/MWCNTs on a supported catalyst is a key issue. For CNT growth without a sulfur containing additive in the CVD process, the diameter of the CNT is closely related to the size of the catalysts. For a supported catalyst, the metal will get sintered into nanoparticles at the high temperature needed for CNT growth. The amount of metal on a fluidizable porous support should be delicately controlled for the highly selective synthesis of CNTs with a controlled wall number and diameter.

In the present work, MgO-supported Fe was used as the model catalyst to investigate the effect of iron loading on the formation of S/D/MWCNTs. Scanning electron microscopy (SEM), high-resolution transmission electron microscopy (TEM), Raman spectroscopy, and thermogravimetric analysis (TGA) were used to characterize the products to study the growth mechanism of the selective growth of CNTs. This provides a high quality catalyst and general understanding for the large scale selective synthesis of CNTs in a fluidized bed reactor.

1 Experimental

1.1 Porous Fe/MgO catalyst preparation

The porous MgO-supported Fe catalyst was prepared by a typical impregnation method. The porous magnesium oxide powder (BET surface area 25.9 m^2/g) was suspended in distilled water to form a uniform suspension by strong stirring at 80 °C. $Fe(NO_3)_3·9H_2O$, purchased from Beijing Yili Reactant Company, was also dispersed in deionized water. Then the solution of iron nitrate was added dropwise slowly into the suspension with stirring. The molar ratio of the salt in the solution to the magnesium oxide was controlled by the amount of the solution added into the MgO suspension. After sonication for 10 min, hydrothermal treatments were performed at a temperature of 200 °C for 2 h. Then the solution was cooled to room temperature. After drying the suspension and grinding the solid, the catalyst of Fe/porous MgO for CNT production was obtained. The Fe amounts on the different catalysts were controlled at 0.5%, 1.0%, 3.0%, 5.0%, and 15.0%.

1.2 CNT growth via chemical vapor deposition

To synthesize the CNTs, approximately 100 mg of the catalyst was sprayed uniformly into a quartz boat, which was then inserted into the center of a quartz tube (i.d. 35 mm, length 1200 mm). The quartz tube, mounted in an electrical tube furnace, was heated to 900 °C in the air atmosphere. Subsequently, argon was fed at a flow rate of 600 ml/min for 60 min. A mixture of methane (80 ml/min) and carrier gas was introduced into the quartz tube and maintained at the reaction temperature for 15 min before the furnace was cooled to room temperature under Ar protection.

1.3 Characterization

The morphology of the CNTs was characterized by SEM (JSM 7401F at 3.0 kV). The sample for TEM was prepared by the sonication of about 5.0 mg of the as-grown products in ethanol and several drops were dropped onto a TEM grid. The quality of the sample was characterized by TEM (JEM 2010 at 120.0 kV). Raman experiments were performed on a Raman spectrophotometer (Renishaw RM2000) at ambient condition. The spectra were recorded using He-Ne laser excitation lines of 514 and 633 nm with a spot size of about 20 μm^2 on the CNTs kept at ambient temperature. The carbon content was obtained by TGA (Q500, heated at 20 °C/min).

2 Results and discussion

2.1 Morphology of the as grown products

Typical SEM images of the products are shown in Fig. 1. The as-grown products were agglomerates with an average size of ca 15 μm, which consisted of CNTs and MgO particles (Fig. 1(a)). In the high magnification SEM images shown in Fig. 1(b), fibrous CNTs can be found among the catalyst particles. The CNTs grown on 0.5%Fe/MgO were in the holes of the MgO catalyst, but the amount was limited. Furthermore, the diameter of the CNTs was small. With increasing iron loading, more CNTs were found on the surface and in the pores of the catalysts (Fig. 1(c)–(e)). The diameter of the CNT bundles became large. CNTs entangled into a woven-structure on the surface of the catalyst were found when the loading was increased to 5% (Fig. 1(e)). However, when the loading was increased to 15%, the density of CNTs decreased (Fig. 1(f)).

2.2 Structure of the as-grown products

In order to macroscopically characterize the structural difference of the as-grown CNTs on the 0.5%–15%Fe/MgO catalysts, Raman spectra were used (Fig. 2). The presence of the radial breath modes (RBM) in the low wavenumber region (100–300 cm^{-1}) indicates the existence of SWCNT or DWCNT in the products. The Kataura plot is attached to the top of the figure [34], in which solid circles represent metallic SWCNTs, and hollow circles and squares show semi-conductive SWCNTs [35,36]. It was noticed that when the incident laser energy changed, the resonance RBM peak positions also changed. With 514 nm laser as the incident beam, there were

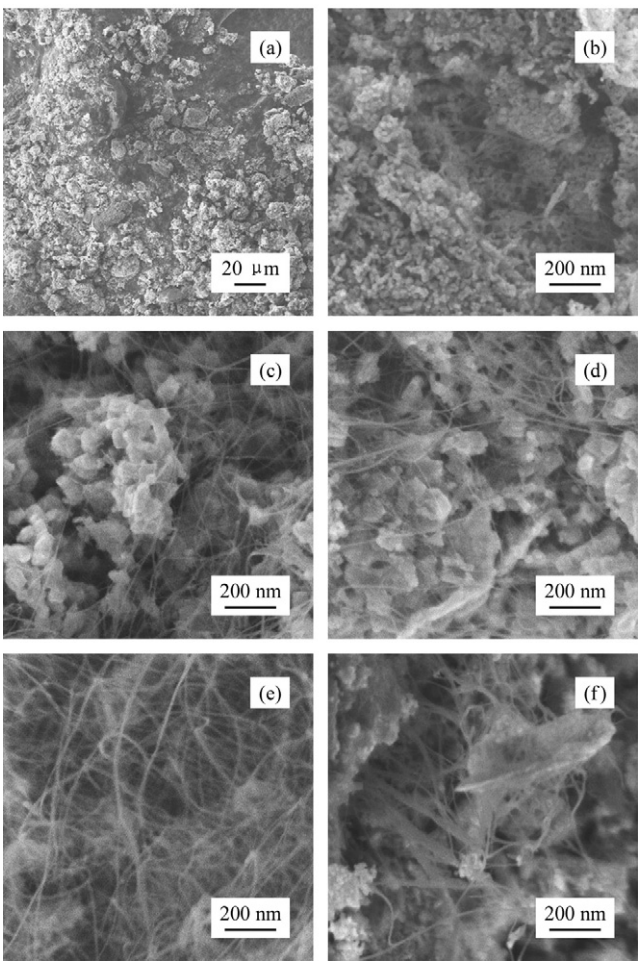

Fig. 1. SEM images of as-grown CNTs from methane over Fe/MgO catalysts at 900 °C. (a) Agglomerated structure of the CNTs; (b) 0.5%Fe/MgO; (c) 1.0%Fe/MgO; (d) 3.0%Fe/MgO; (e) 5.0%Fe/MgO; (f) 15.0%Fe/MgO.

peaks at 134, 165, 184, 222, and 266 cm^{-1}, which were due to metallic, semi-conductive, semi-conductive, metallic, and semi-conductive nanotubes, respectively. But the amount of CNTs of a specific diameter was different.

As shown in Fig. 2(a), the peak at 134 cm^{-1} increased, while the peak at 184 and 266 cm^{-1} clearly decreased. This indicated that with increasing iron loading on the MgO supports, the diameter of as-grown CNT increased. Furthermore, the peaks at 134, 165, and 184 cm^{-1} were the main RBM peaks for the products grown on a highly loaded catalyst, indicating that the relative amount of semiconductor CNT increased. From the Raman spectra of the as-grown CNTs with the 633 nm laser as the incident beam, the peak at the higher wavenumber decreased, which indicated that the amount of small diameter CNTs decreased. Furthermore, the area ratio of the peaks at 140 and 191 cm^{-1} still increased, indicating the higher proportion of semiconducting CNTs [35,36]. However, it was noticed that both metallic and semiconductor CNTs could be found from each catalyst. Thus, there is still a long way to go to achieve the selective growth of metallic or semiconductor CNTs.

In addition, typical D and G peaks from the CNTs are shown in Fig. 2(b). The intensity ratio of the D to G peak is proportional to the degree of graphite crystallinity. The values for all the samples were less than 0.19, indicating that the SWCNTs or DWCNTs had a high degree of crystallinity [33,37]. The intensity ratio of the D to G peaks is different with a different incident beam energy, but the trends were similar. However, the trends revealed less information on the defect density because the products were a mixture of SWCNTs, DWCNTs, MWCNTs, and carbon sphere encapsulated particles. Furthermore, the Breit-Wigner-Fano (BWF) peak at around 1500 cm^{-1}, which is a characteristic Raman mode of metallic nanotubes [22], decreased gradually. This indicated that the content of metallic CNTs decreased in the as-grown products with a high iron loading, which is consistent with the RBM peak analysis.

Fig. 3(a) shows a typical TEM image of the as-grown CNTs products on the Fe/MgO catalyst. The CNTs, especially SWCNTs, were clustered into CNT bundles due to the strong van der Waals force. The CNT bundles had a diameter of 3–15 nm. The high resolution TEM images of CNTs grown on Fe/MgO catalysts with different iron loadings are shown in Figs. 3(b)–(f). With increasing iron content, both the wall number and the diameter of the CNTs increased.

The distribution of the wall number is given in Fig. 4. When the iron content was 0.5%, about 90% CNTs had a single wall, and the mean diameter was 1.87 nm. When the iron content was increased to 1.0%, the content of SWCNTs decreased to 65%, while DWCNTs and three-walled CNTs clearly increased and the mean diameter increased to 2.02 nm. DWCNTs with a selectivity of 75% could be obtained when the iron loading was 3.0%. When the iron amount was increased to 15.0%, both the wall number and diameter distribution of CNTs in the as-grown products increased (Fig. 3(f), Fig. 4, and Fig. 5). MWCNTs were the main products while SWCNTs and DWCNTs still existed, so the RBM peak was still present as shown in Fig. 2(a).

The yield of CNTs can be obtained from a TGA test. The weight loss during TGA is shown in Fig. 6. With increasing iron content, the carbon content clearly increased, indicating that more carbon was deposited on the Fe/MgO catalyst. On the assumption that only CNTs were deposited on the catalyst, and the Fe particles were oxidized to Fe_2O_3 during TGA, we defined the carbon yield on the basis of the active site. Thus, the carbon yield was the mass ratio of the CNTs grown to the iron catalyst. It can be used to evaluate the active sites for CNT growth on the iron catalyst. When the iron loading was 0.5%, only 5% carbon was deposited on the catalyst. However, the mass of carbon produced was 19 times that of the active phase, which was obviously higher than that on the 5.0%Fe/MgO and 15.0%Fe/MgO catalysts. The carbon yield exhibited an opposite trend to the carbon content.

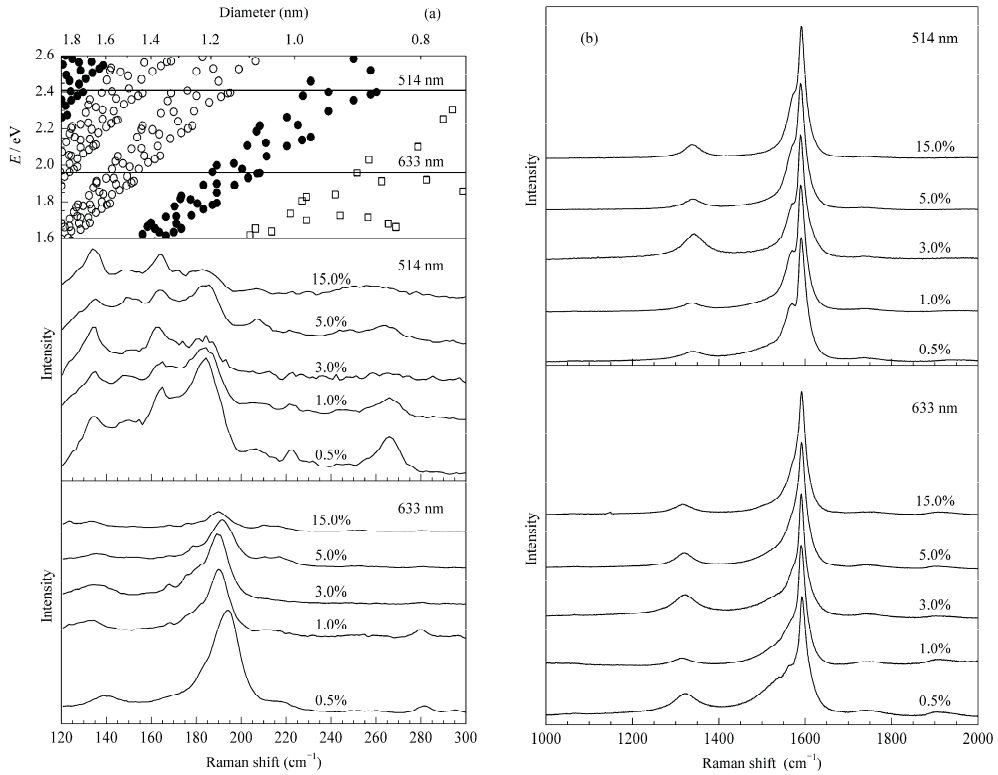

Fig. 2. Raman spectra of as-grown CNTs from methane on Fe/MgO catalyst at 900 °C. (a) RBMs of the as-grown product excited with 514 and 633 nm lasers (The Kataura plot is attached to the top of the figure [34], in which solid circles represent metallic SWNTs, squares are from Weisman [35] and hollow circles are from Maruyama [36]. The diameter was calculated by $\omega_{RBM} = 223.8/d_t$.; (b) D and G peaks of the as-grown product excited with 514 nm and 633 nm lasers.

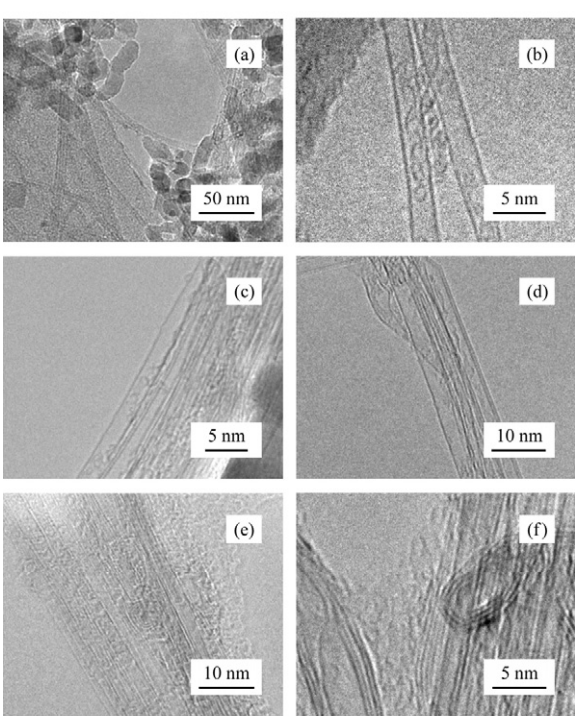

Fig. 3. TEM images of as-grown CNTs from methane on Fe/MgO catalysts at 900 °C. (a) Agglomerated structure of CNTs; (b) 0.5%Fe/MgO; (c) 1.0%Fe/MgO; (d) 3.0%Fe/MgO; (e) 5.0%Fe/MgO; (f) 15.0%Fe/MgO.

2.3 Growth mechanism

Based on the above evidence, it was concluded that S/D/MWCNTs were selectively synthesized on Fe/MgO catalysts with different loadings. The growth mechanism for selective growth can be explained by the vapor-liquid-solid (VLS) model [38]. During catalyst impregnation and hydrothermal treating, the iron atoms were dispersed on the MgO carrier. After calcination and the introduction of methane, the iron atoms began to sinter into iron particles. Then methane can be adsorbed and catalytically decomposed into carbon and hydrogen on the surface of the iron particles. This is followed by the diffusion of carbon into the metal particles until the bulk became saturated; when supersaturation occurred, precipitation of carbon nanotubes occurred from the metal surface under proper conditions. There is a strong metal support interaction between Fe and MgO [21,22]. Fe can dissolve in MgO and disperse uniformly after a hydrothermal process [24]. At higher temperatures, iron will precipitate from the MgO and forms small particles, especially in the presence of hydrogen [21–23]. If the iron amount was 0.5%, the iron formed small Fe iron particles with a size of about 0.8–1.2 nm (Fig. 7(a)). Since the size of the iron particle was small, the dominating surface diffusion on the catalyst particle resulted in the formation of SWCNT [13,14,17]. When the iron loading was increased to 3.0%, the iron atoms were sintered into large iron particles with

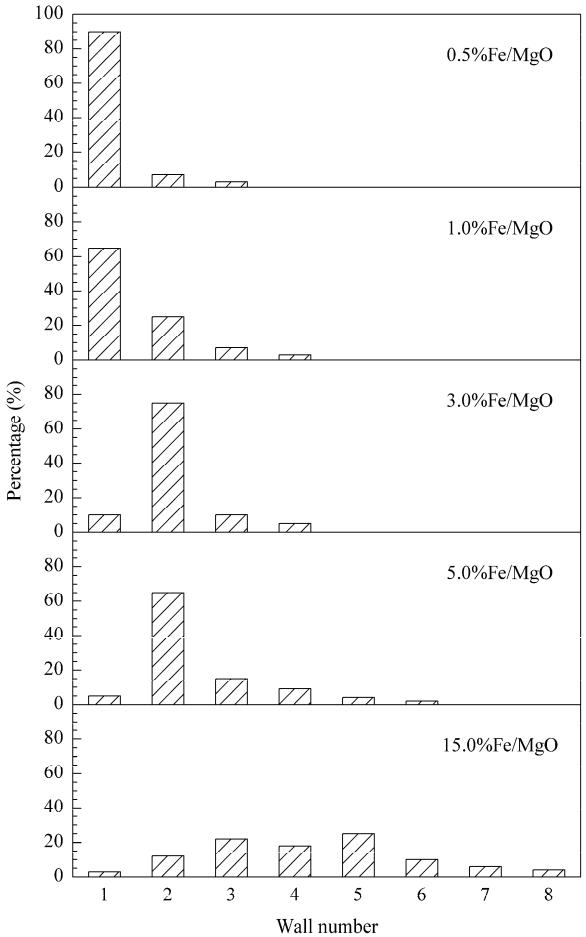

Fig. 4. Wall number distribution of the as-grown CNTs from methane on the various Fe/MgO catalysts at 900 °C.

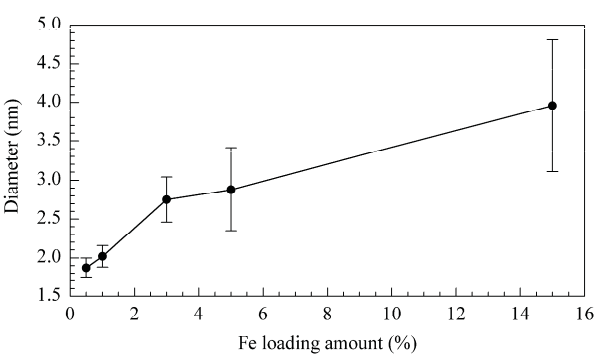

Fig. 5. Diameter of the as-grown CNTs from methane on the various Fe/MgO catalysts at 900 °C.

a size of 2.0 nm (Fig. 7(b)). Both surface and bulk diffusion, which contributed to the outer and inner layer of DWCNT formation, respectively, took place on a single particle. Thus, DWCNTs were the main products for the CNTs grown on the 3%Fe/MgO catalyst. When the catalyst loading was increased further, the size of the catalyst particle had a large range of 1-8 nm. According to the VLS model, the diameter distribution of the as-grown CNTs on these particles was relatively broad as shown in Fig. 5. For the large particles, the bulk diffusion of

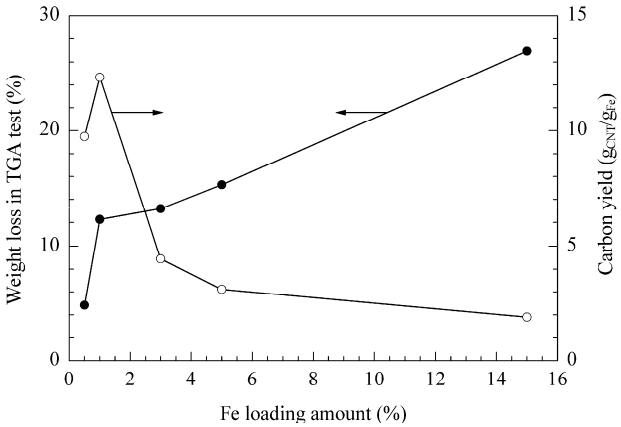

Fig. 6. Weight loss in the TGA test and carbon yield versus iron loading for CNTs grown on the Fe/MgO catalysts.

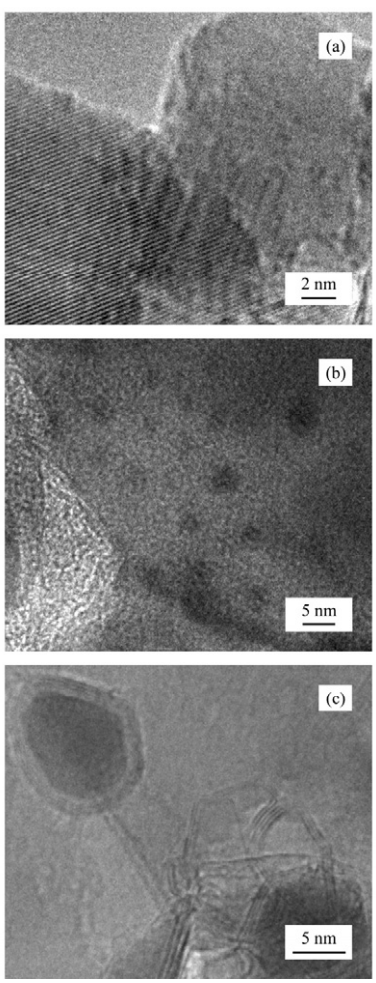

Fig. 7. Catalyst particle on the 0.5%Fe/MgO (a), 3.0%Fe/MgO (b), and 15.0%Fe/MgO (c) catalysts.

carbon dominated in the synthesis of CNTs. Due to the low activity of the large iron catalyst, carbon atoms can accumulate at the surface of the catalyst and encapsulate the iron catalyst into a tubular structure (Fig. 7(c)). Thus, the carbon yield decreased due to the low efficiency of CNT growth on the large iron catalyst particles (Fig. 6).

3 Conclusions

S/D/MWCNTs were selectively synthesized using Fe/MgO catalysts with different iron loading. When the iron loading was low, iron atoms distributed on the MgO catalyst sintered into iron particles with a size of 0.8–1.2 nm, and SWCNTs were formed on these by the surface diffusion of carbon atoms. The selectivity for SWCNTs on 0.5%Fe/MgO was over 90%. The mass of carbon produced was 19 times that of the active phase on this catalyst. When the iron loading was increased to 3%, larger iron catalyst particles with a size of ca. 2 nm were formed. Due to the added presence of the bulk diffusion of carbon, DWCNTs were the main products for the combination of surface and bulk diffusion. When the iron loading was further increased, iron particles with a size distribution of 1–8 nm were formed. MWCNTs together with S/DWCNTs were synthesized on these. The diameter distribution, wall number and proportion of semiconducting CNTs increased with the amount of iron supported on MgO. The selective synthesis of metallic or semiconducting CNTs is still a challenge. Since the porous Fe/MgO catalyst in this work can be easily fluidized, we have provided an approach for the large scale selective synthesis of S/D/MWCNTs for further potential applications.

References

[1] Serp P, Corrias M, Kalck P. *Appl Catal A*, 2003, **253**(2): 337

[2] Chen W, Pan X L, Willinger M G, Su D S, Bao X H. *J Am Chem Soc*, 2006, **128**(10): 3136

[3] Delgado J J, Vieira R, Rebmann G, Su D S, Keller N, Ledoux M J, Schlogl R. *Carbon*, 2006, **44**(4): 809

[4] Pan X L, Fan Z L, Chen W, Ding Y J, Luo H Y, Bao X H. *Nature Mater*, 2007, **6**(7): 507

[5] Li P, Li T, Zhou J H, Sui Z J, Dai Y C, Yuan W K, Chen D. *Microporous Mesoporous Mater*, 2006, **95**(1–3): 1

[6] Fan S S, Chapline M G, Franklin N R, Tombler T W, Cassell A M, Dai H J. *Science*, 1999, **283**(5401): 512

[7] Yao Y G, Li Q W, Zhang J, Liu R, Jiao L Y, Zhu Y T, Liu Z F. *Nature Mater*, 2007, **6**(4): 283

[8] Cheng H M, Li F, Sun X, Brown S D M, Pimenta M A, Marucci A, Dresselhaus G, Dresselhaus M S. *Chem Phys Lett*, 1998, **289**(5–6): 602

[9] Zhou Z P, Ci L J, Song L, Yan X Q, Liu D F, Yuan H J, Gao Y, Wang J X, Liu L F, Zhou W Y, Wang G, Xie S S. *Carbon*, 2003, **41**(13): 2607

[10] Wei J Q, Zhu H W, Jia Y, Shu Q K, Li C G, Wang K L, Wei B Q, Zhu Y Q, Wang Z C, Luo J B, Liu W J, Wu D H. *Carbon*, 2007, **45**(11): 2152

[11] Liu Q F, Ren W C, Chen Z G, Wang D W, Liu B L, Yu B, Li F, Cong H T, Cheng H M. *ACS Nano*, 2008, **2**(8): 1722

[12] Wei F, Zhang Q, Qian W Z, Yu H, Wang Y, Luo G H, Xu G H, Wang D Z. *Powder Technol*, 2008, **183**(1): 10

[13] Dal H J, Rinzler A G, Nikolaev P, Thess A, Colbert D T, Smalley R E. *Chem Phys Lett*, 1996, **260**(3–4): 471

[14] Nikolaev P, Bronikowski M J, Bradley R K, Rohmund F, Colbert D T, Smith K A, Smalley R E. *Chem Phys Lett*, 1999, **313**(1–2): 91

[15] Wang Y, Wei F, Luo G H, Yu H, Gu G S. *Chem Phys Lett*, 2002, **364**(5–6): 568

[16] Zhang Q, Qian W Z, Wen Q, Liu Y, Wang D H, Wei F. *Carbon*, 2007, **45**(8): 1645

[17] Wang Y Y, Gupta S, Nemanich R J. *Appl Phys Lett*, 2004, **85**(13): 2601

[18] Yu H, Zhang Q, Zhang Q F, Wang Q X, Ning G Q, Luo G H, Wei F. *Carbon*, 2006, **44**(9): 1706

[19] Li Q W, Yan H, Cheng Y, Zhang J, Liu Z F. *J Mater Chem*, 2002, **12**(4): 1179

[20] Liu J X, Ren Z, Duan L Y, Xie Y C. *Acta Chim Sinica*, 2004, **62**(8): 775

[21] Ago H, Nakamura K, Uehara N, Tsuji M. *J Phys Chem B*, 2004, **108**(49): 18908

[22] Ago H, Imamura S, Okazaki T, Saitoj T, Yumura M, Tsuji M. *J Phys Chem B*, 2005, **109**(20): 10035

[23] Ning G Q, Wei F, Wen Q, Luo G H, Wang Y, Jin Y. *J Phys Chem B*, 2006, **110**(3): 1201

[24] Ning G Q, Liu Y, Wei F, Wen Q, Luo G H. *J Phys Chem C*, 2007, **111**(5): 1969

[25] Wen Q, Qian W Z, Wei F. *Chin J Catal*, 2008, **29**(7): 617

[26] Lyu S C, Liu B C, Lee C J, Kang H K, Yang C W, Park C Y. *Chem Mater*, 2003, **15**(20): 3951

[27] Hart A J, Slocum A H, Royer L. *Carbon*, 2006, **44**(2): 348

[28] Lamouroux E, Serp P, Kihn Y, Kalck P. *Catal Commum*, 2006, **7**(8): 604

[29] Lyu S C, Liu B C, Lee S H, Park C Y, Kang H K, Yang C W, Lee C J. *J Phys Chem B*, 2004, **108**(7): 2192

[30] Li Y, Zhang X B, Shen L H, Xu J M, Liu F, Xu G L, Wang Y W. *Chin J Chem Phys*, 2005, **18**(3): 411

[31] Zhang H, Shin D H, Lee H S, Lee C J. *J Phys Chem C*, 2007, **111**(35): 12954

[32] Gruneis A, Rummeli M H, Kramberger C, Barreiro A, Pichler T, Pfeiffer R, Kuzmany H, Gemming T, Buchner B. *Carbon*, 2006, **44**(15): 3177

[33] Zhang Q, Yu H, Liu Y, Qian W Z, Wang Y, Luo G H, Wei F. *Nano*, 2008, **3**(1): 45

[34] Kataura H, Kumazawa Y, Maniwa Y, Umezu I, Suzuki S, Ohtsuka Y, Achiba Y. *Synthetic Met*, 1999, **103**(1–3): 2555

[35] Weisman R B, Bachilo S M. *Nano Lett*, 2003, **3**(9): 1235

[36] Maruyama S, Murakami Y, Shibuta Y, Miyauchi Y, Chiashi S. *J Nanosci Nanotech*, 2004, **4**(4): 360

[37] Qian W Z, Liu T, Wei F, Yuan H Y. *Carbon*, 2003, **41**(9): 1851

[38] Baker R T K, Harris P S, Thomas R B, Waite R J. *J Catal*, 1973, **30**(1): 8